Resolving Heterogeneity on the Single Molecular Level with the Photon-Counting Histogram

Joachim D. Müller, Yan Chen, and Enrico Gratton
Laboratory for Fluorescence Dynamics, University of Illinois at Urbana–Champaign, Urbana, Illinois, 61801 USA

ABSTRACT The diffusion of fluorescent particles through a small, illuminated observation volume gives rise to intensity fluctuations caused by particle number fluctuations in the open observation volume and the inhomogeneous excitation-beam profile. The intensity distribution of these fluorescence fluctuations is experimentally captured by the photon-counting histogram (PCH). We recently introduced the theory of the PCH for diffusing particles (Chen et al., *Biophys. J.*, 77:553–567), where we showed that we can uniquely describe the distribution of photon counts with only two parameters for each species: the molecular brightness of the particle and the average number of particles within the observation volume. The PCH is sensitive to the molecular brightness and thus offers the possibility to separate a mixture of fluorescent species into its constituents, based on a difference in their molecular brightness alone. This analysis is complementary to the autocorrelation function, traditionally used in fluorescence fluctuation spectroscopy, which separates a mixture of species by a difference in their diffusion coefficient. The PCH of each individual species is convoluted successively to yield the PCH of the mixture. Successful resolution of the histogram into its components is largely a matter of the signal statistics. Here, we discuss the case of two species in detail and show that a concentration for each species exists, where the signal statistics is optimal. We also discuss the influence of the absolute molecular brightness and the brightness contrast between two species on the resolvability of two species. A binary dye mixture serves as a model system to demonstrate that the molecular brightness and the concentration of each species can be resolved experimentally from a single or from several histograms. We extend our study to biomolecules, where we label proteins with a fluorescent dye and show that a brightness ratio of two can be resolved. The ability to resolve a brightness ratio of two is very important for biological applications.

INTRODUCTION

The development of confocal and multiphoton spectroscopy has given us the opportunity to measure fluorescence from very small sample volumes (Qian and Elson, 1991; Rigler et al., 1993a; Berland et al., 1995). The reduction of the sample volume by more than nine orders of magnitude, compared to conventional fluorescence techniques, leads to an equal reduction in the number of particles present in the observation volume. In fact, the observation of single molecules has been achieved with these small volumes (Rigler et al., 1993b; Eigen and Rigler, 1994). The small number of molecules diffusing through the observation volume causes large intensity fluctuations of the fluorescence signal.

This appearance of fluorescence intensity fluctuations can be exploited as an additional source of information to determine kinetic properties associated with the particles (Elson and Magde, 1974). The original experiments conducted by Webb and coworkers (Magde et al., 1972, 1974) started a new field, which is known as fluorescence correlation spectroscopy (FCS). After more than two decades of development, FCS has matured enough so that it is now quite commonly used to investigate processes on the molecular level (Bonnet et al., 1998; Haupts et al., 1998). FCS has been used to study a variety of processes, such as translational diffusion (Koppel et al., 1976), chemical reactions (Magde, 1976), rotational diffusion (Ehrenberg and Rigler, 1974), protein oligomerization (Berland et al., 1996), triplet-state kinetics (Widengren et al., 1995), surface and bulk processes (Borejdo, 1979; Thompson and Axelrod, 1983), membrane surfaces (Huang and Thompson, 1996), and others (Magde et al., 1978; Weissman et al., 1976). Here, we use the terms particle and molecule interchangeably. In our context, particle refers to a fluorescent, point-like object.

Statistical considerations require that only a small number of particles be present in the observation volume at any instance of time to observe the intensity fluctuations generated by individual particles. The methods of data analysis at or close to the single molecule level are quite different from the methods used to characterize particle ensembles in bulk solutions. The fluctuations inherent in the measured signal mandate the use of statistical methods to analyze the data. For example, FCS uses the autocorrelation function of the intensity fluctuations to characterize the time-dependent decay of these fluctuations to their equilibrium value.

The use of small sample volumes, together with the ability to measure processes close to the single molecule level in vitro or in vivo, make FCS attractive for the study of biological systems. However, biological macromolecules interact with other molecules as part of a network, which maintains the complex machinery of life. Thus, almost every biological system of interest consists of more than a single species, and we have to consider how to separate components of a mixture on the single-molecule level. FCS

Received for publication 22 June 1999 and in final form 20 October 1999.
Address reprint requests to Joachim D. Müller, 184 Loomis Laboratory, Laboratory for Fluorescence Dynamics, 1110 West Green, Urbana, IL 61801. Tel.: 217-244-5620; Fax: 217-244-7187; E-mail: muller@uiuc.edu.

0006-3495/00/01/474/13 $2.00

has been applied successfully in resolving species based on their diffusion coefficients (Rauer et al., 1996; Klingler and Friedrich, 1997). However, to separate two species by the autocorrelation analysis requires a difference in their translational diffusion coefficients by approximately a factor of two (Meseth et al., 1999), which corresponds to a molecular weight difference of about eight. Unfortunately, quite a number of important processes do not produce such a large change in the molecular weight. For example, the formation of a dimer from two monomers leads to a change of the diffusion coefficient of only 25%. Thus, a mixture of monomers and dimers cannot be resolved by the autocorrelation function alone.

To address this shortcoming of the autocorrelation approach, methods have been introduced to separate species based on molecular brightness rather than molecular weight. Higher-order autocorrelation and moments analyses use the information of higher moments to separate species (Palmer and Thompson, 1987; Qian and Elson, 1990b). Here, we propose a different method, which exploits the distribution of photon counts to separate species by their molecular brightness. Molecular brightness is the fluorescence intensity produced by a single particle in the observation volume and depends on the physical properties of the dye and the detection setup. The concept is quite straightforward. A particle with a given brightness produces a characteristic intensity fluctuation as it traverses through the observation volume. If another particle with a higher molecular brightness enters the observation volume, this event is accompanied by a stronger intensity fluctuation in the fluorescence signal. The statistics of the amplitudes of the intensity fluctuations will capture the distribution of molecular brightness values and their recurrence frequency. Thus, the amplitude statistics provides a quantitative description of the molecular brightnesses of the particles together with their respective concentrations.

So far, we have described the basic concept and omitted a few complicating factors: 1) We observe an open system with particles entering and leaving the observation volume. Therefore, the particle number fluctuation occurring in such a system must be taken explicitly into account. 2) The illumination profile of the excitation volume is inhomogeneous, thus leading to a distribution of fluorescent intensities, which depends on the actual shape of the beam profile. 3) Last, but not least, we detect discrete photon counts instead of intensities. The photodetection process adds another layer of noise to the signal and changes the signal statistics (Saleh, 1978). Thus, to separate species by their molecular brightness, we need to know how these three factors contribute to the observed amplitude statistics.

In a recent publication, we developed a theoretical expression for the photon-counting histogram (PCH), which takes the inhomogeneous excitation profile, the particle number fluctuations, and the detection process into account (Chen et al., 1999). In that article, we mainly focused on the behavior of a single species. Here, in contrast, we explore the use of the PCH to separate species based on a difference in their molecular brightness. We discuss the resolvability and sensitivity of the PCH in separating two species as a function of the sample conditions, such as the molecular brightness and the particle concentration. A binary dye mixture serves as a model system to test experimentally the resolvability of two species by the PCH. We also study biomolecules labeled with either one or two fluorescent dyes and resolve the mixture by PCH analysis.

THEORY

The PCH captures the amplitude distribution of the intensity fluctuations (Mandel, 1958). The intensity profile of the observation volume created by confocal or two-photon techniques are described by their respective point spread functions (PSFs) (Qian and Elson, 1991; Berland et al., 1995). We define a scaled point spread function $\overline{\mathrm{PSF}}$, so that the volume of the scaled PSF, $V_{\mathrm{PSF}} = \int \overline{\mathrm{PSF}}(\vec{r})\, d\vec{r}$, equals the volume definition of FCS experiments (Thompson, 1991). Because the PSF is inhomogeneous, particles moving inside the PSF give rise to intensity fluctuations.

For a single particle, diffusing within a small box of volume V_0 that encloses the observation volume, these intensity fluctuations lead to the following photon count distribution (Chen et al., 1999),

$$\mathrm{p}^{(1)}(k; V_0, \epsilon) = \int \mathrm{Poi}(k, \epsilon\overline{\mathrm{PSF}}(\vec{r}))\mathrm{p}(\vec{r})\, d\vec{r}, \qquad (1)$$

where $\mathrm{Poi}(k, \mu)$ is the Poisson distribution with expectation value μ. The probability $\mathrm{p}^{(1)}(k; V_0, \epsilon)$ for observing k photon counts for a single particle depends on the reference volume V_0 and the parameter ϵ. The function $\mathrm{p}(\vec{r})$ describes the probability to find the particle at position $\vec{r}$. For a particle immobilized at position $\vec{r}_0$, Eq. 1 reduces to a Poisson distribution,

$$\mathrm{p}^{(1)}_{\mathrm{fixed}}(k) = \mathrm{Poi}(k, \epsilon\overline{\mathrm{PSF}}(\vec{r}_0)) = \frac{(\epsilon\overline{\mathrm{PSF}}(\vec{r}_0))^k \exp[-\epsilon\overline{\mathrm{PSF}}(\vec{r}_0)]}{k!}. \qquad (2)$$

It is the shot noise generated by the detection process of the constant fluorescence intensity of the immobilized particle that gives rise to the above Poisson distribution (Saleh, 1978). However, we are interested in a freely diffusing particle, in which the probability $\mathrm{p}(\vec{r})$ to find the particle at any position within the volume of the reference box is equal to $1/V_0$ and outside of it is equal to zero.

The physical meaning of the parameter ϵ becomes clear if we calculate the average photon counts $\langle k \rangle$ for a diffusing

particle according to Eq. 1,

$$\langle k\rangle = \frac{\epsilon}{V_0}\int_{V_0} \overline{\mathrm{PSF}}(\vec{r})\,\mathrm{d}\vec{r} = \epsilon\,\frac{V_{\mathrm{PSF}}}{V_0}. \qquad (3)$$

Thus, the average photon counts are determined by the product of ϵ and the probability to find the molecule within the volume of the point spread function V_{PSF}. Therefore ϵ describes the molecular brightness, which determines the average number of photon counts received during the sampling time Δt_s for a particle within the observation volume V_{PSF}. The average photon counts received $\langle k\rangle$ scale linearly with the sampling time. Therefore, the detected photon rate $\epsilon_{\mathrm{sec}} = \epsilon/\Delta t_s$ is independent from the somewhat arbitrary sampling time Δt_s. The parameter ϵ_{sec} expresses the molecular brightness in photon counts per second per molecule (cpsm) and allows a more convenient comparison between different experiments.

Now let us consider N independent and identical particles diffusing inside a box of volume V_0. If one could follow one particular particle individually, the PCH of this particle would be given by $\mathrm{p}^{(1)}(k; V_0, \epsilon)$ according to Eq. 1. For N independent particles, the corresponding PCH, $\mathrm{p}^{(N)}(k; V_0, \epsilon)$, is given by consecutive convolutions of the single particle PCH functions $\mathrm{p}^{(1)}(k; V_0, \epsilon)$ (Feller, 1957),

$$\mathrm{p}^{(N)}(k; V_0, \epsilon) = \underbrace{(\mathrm{p}^{(1)} \otimes \cdots \otimes \mathrm{p}^{(1)})}_{\text{N-times}}(k; V_0, \epsilon). \qquad (4)$$

Of course, if there are no particles in the reference volume, no photon counts are generated and we define the corresponding PCH as,

$$\mathrm{p}^{(0)}(k; V_0, \epsilon) = \delta(k), \quad \text{with} \quad \delta(k) = \begin{cases} 1, & k = 0 \\ 0, & k > 0. \end{cases} \qquad (5)$$

The assumption of a closed system, in which particles diffuse inside a box, does not describe the experimental situation, unless the reference volume includes the whole sample. But a macroscopic reference volume would require the evaluation of an astronomical number of convolutions according to Eq. 4. Instead, we choose to consider an open system in which particles are allowed to enter and leave a small subvolume. The subvolume is in contact with a much larger reservoir volume and the distribution of the number of particles N inside the subvolume is given by a Poisson distribution (Chandrasekhar, 1943),

$$\mathrm{p}_{\#}(N) = \mathrm{Poi}(N, \bar{N}), \qquad (6)$$

where $\bar{N}$ describes the average number of molecules within the reference volume V_0. We point out that this Poisson distribution has a different physical origin than the shot noise, which is due to the detection process.

Now we can express the PCH for an open system $\hat{\mathrm{p}}(k; V_0, \bar{N}, \epsilon)$ as the expectation value of the N-particle PCH $\mathrm{p}^{(N)}(k; V_0; \epsilon)$, considering Poissonian number statistics,

$$\Pi(k; \bar{N}_{\mathrm{PSF}}, \epsilon) \equiv \hat{\mathrm{p}}(k; V_0, \bar{N}, \epsilon) = \langle \mathrm{p}^{(N)}(k; V_0, \epsilon)\rangle_{\mathrm{N}}. \qquad (7)$$

The PCH function $\hat{\mathrm{p}}(k; V_0, \bar{N}, \epsilon)$ describes the probability of observing k photon counts per sampling time for an open system with an average of $\bar{N}$ particles inside the reference volume V_0.

The particular choice of the reference volume for an open system is irrelevant. It is intuitively clear that the properties of an open system have to be independent of the arbitrary reference volume V_0 (Chen et al., 1999). Thus, the photon-count distribution should either be referenced to an intensive quantity, like the particle concentration, or to some standard volume. We choose the convention used in FCS, where the volume of the PSF, V_{PSF}, connects the $g(0)$ value of the autocorrelation function to the average number of molecules $\bar{N}_{\mathrm{PSF}}$ (Thompson, 1991). Consequently, we drop the V_0 parameter dependence for the PCH of an open system and declare a new function $\Pi(k; \bar{N}_{\mathrm{PSF}}, \epsilon)$, which characterizes the PCH of an open system referenced to the volume of the PSF. The average number of photon counts $\langle k\rangle$ can be calculated from Eq. 7 and is given by the product of the molecular brightness ϵ and the average number of particles $\bar{N}_{\mathrm{PSF}}$ inside the PSF volume,

$$\langle k\rangle = \epsilon\bar{N}_{\mathrm{PSF}}. \qquad (8)$$

So far, only identical particles have been treated. Often more than one type of particle is present in the sample. It is straightforward to expand the theory under the assumption that the particles are noninteracting. Let us consider the case of two different species for simplicity. If we could distinguish the photon counts emerging from each species, we could directly determine the PCH of each species, $\Pi(k; \bar{N}_1, \epsilon_1)$ and $\Pi(k; \bar{N}_2, \epsilon_2)$. However, because we are assuming that the particles have identical spectral properties, we cannot distinguish the origin of the photon counts. However, as long as the photon emission of both species is statistically independent, the PCH of the mixture is given by the convolution of the photon count distributions of species 1 with that of species 2,

$$\Pi(k; \bar{N}_1, \bar{N}_2, \epsilon_1, \epsilon_2) = \Pi(k; \bar{N}_1, \epsilon_1) \otimes \Pi(k; \bar{N}_2, \epsilon_2). \qquad (9)$$

For more than two species, all single-species photon-counting distributions are convoluted successively to yield the photon-count distribution of the mixture.

The photon-count distribution depends on the PSF. Here, we report the PCH of a single particle $\mathrm{p}^{(1)}(k; V_0, \epsilon)$ for the Gaussian–Lorentzian squared PSF, which has been used to describe the two-photon excitation beam profile for our experimental conditions (Berland et al., 1995),

$$\overline{\mathrm{PSF}}_{2\mathrm{GL}}(\rho, z) = \frac{4\omega_o^4}{\pi^2\omega^4(z)}\exp\left[-\frac{4\rho^2}{\omega^2(z)}\right]. \qquad (10)$$

The PSF is expressed in cylindrical coordinates and the excitation profile has a beam waist ω_0. The inverse of the Lorentzian along the optical axis for an excitation wavelength of λ is given by,

$$\omega^2(z) = \omega_o^2\left(1 + \left(\frac{z}{z_R}\right)^2\right), \quad \text{with} \quad z_R = \frac{\pi\omega_o^2}{\lambda}. \qquad (11)$$

To calculate the PCH of a single particle for a reference volume V_0, $p(\vec{r})$ is set equal to $1/V_0$, Eq. 10 is inserted into Eq. 1, and then integrated over all space. Integrating over all space is mathematically convenient and ensures the correct PCH for the open volume case, because, from a mathematical point of view, the PSF extends to infinity. However, the PCH of a closed volume is only approximately determined. The quality of the approximation depends on the size of the reference volume V_0. If the volume is chosen so that the contribution of the PSF to the photon counts outside of the reference volume is negligible, then the deviation between the two functions is small. The PCH of a closed volume is, from a practical point of view, only of minor interest, because the experimental situation is described by the PCH of an open volume. We refer the interested reader to a more detailed discussion of this point by Chen et al. (1999). The PCH of a single particle is then determined for $k > 0$ by a one-dimensional integral,

$$p_{2GL}^{(1)}(k; V_0, \epsilon) = \frac{1}{V_0}\frac{\pi^2\omega_o^4}{2\lambda k!}\int_0^\infty (1 + x^2)\gamma\left(k, \frac{4\epsilon}{\pi^2(1 + x^2)^2}\right) dx,$$

$$\text{for } k > 0. \qquad (12)$$

The integral, which contains the incomplete gamma function γ (Abramowitz and Stegun, 1965), can be evaluated numerically.

MATERIALS AND METHODS

Instrumentation

The instrumentation for two-photon fluorescence fluctuation experiments is similar to that described by Berland et al. (1995) with a few modifications. A mode-locked Ti:sapphire laser (Mira 900, Coherent, Palo Alto, CA) pumped by an intracavity doubled Nd:YVO_4 laser (Coherent Inc., Santa Clara, CA) was used as the two-photon excitation source. The experiments were carried out using a Zeiss Axiovert 135 TV microscope (Thornwood, NY) with a 40× Fluar oil immersion objective (N.A. = 1.3). An excitation wavelength in the range from 770 to 780 nm was used for all measurements. The average power at the sample ranged from 10 to 20 mW. Under our experimental conditions, no photobleaching was detected for any of the samples measured. Photon counts were detected with an avalanche photodiode (APD) (EG&G, SPCM-AQ-141). The output of the APD unit, which produces TTL pulses, was directly connected to a home-built data acquisition card. The expected residence time of the molecules inside the excitation beam was used to determine the photon-sampling frequency, which ranged from 20 to 5 kHz. The recorded and stored photon counts were later analyzed with programs written for PV-WAVE version 6.21 (Visual Numerics, Inc., CO) and with LFD Globals Unlimited software (Champaign, IL).

Sample preparation

Rhodamine 110, 3-cyano-7-hydroxycoumarin, and the alexa 488-protein labeling kit were purchased from Molecular Probes (Eugene, OR). All dyes were dissolved in 50 mM Tris[hydroxymethyl]amino-methane (Sigma, MO) and the pH was adjusted to 8.5 by adding HCl. The dye concentration of the stock solutions was determined by optical absorption measurements using the extinction coefficients provided by Molecular Probes. Mouse antialkaline phosphatase monoclonal antibody (IgG) was purchased from Chemicon international (Temecula, CA). The alcohol dehydrogenase was from baker's yeast and contains less than 1% NAD and NADH (Sigma). Both proteins were used for labeling without further purification. The protein-labeling protocol was provided by molecular probes with few modifications. The labeling dye was first dissolved in the labeling buffer to achieve a final concentration of 10 mM. Different amounts of alexa 488 solution were then added to the IgG protein samples to yield concentration ratios of 1:1 for sample A, 25:1 for sample B, and 100:1 for sample C. For the labeling of alcohol dehydrogenase, concentration ratios of 1:1 for sample A and 25:2 for sample B were used. The mixtures of labeling dye and proteins were incubated at room temperature for more than one hour with stirring. In the next step, the mixtures were loaded on G25 Sephadex columns and the samples were collected without further purification. The buffer used for the columns, and subsequently for the fluctuation measurements, was potassium phosphate buffer at 50 mM, pH = 8.4.

Data analysis

The theoretical photon-counting distribution of a single particle $p^{(1)}(k; V_0, \epsilon)$ is directly calculated from Eq. 12. After convoluting the density function $p^{(1)}(k, V_{PSF}, \epsilon)$ according to Eq. 4 to obtain $p^{(N)}(k; V_{PSF}, \epsilon)$, the final probability function for an open system with an average of $\bar{N}$ particles in the reference volume V_{PSF} is determined by weighing $p^{(N)}(k; V_{PSF}, \epsilon)$ according to Eq. 7 with the Poissonian number probability $Poi(N, \bar{N})$.

The histogram of the experimental data is calculated from the recorded photon counts and then normalized to yield the experimental probability density $\tilde{p}(k)$ of k photoelectron counts. A typical data set contains on the order of 10^6 data points, so the values of the photon-counting density $\tilde{p}(k)$ vary over several orders of magnitude. To fit $\tilde{p}(k)$ to the PCH model, we must assign the proper statistical uncertainty to each value of the histogram. For each individual measurement, the probability to yield k counts is given by the probability $\tilde{p}(k)$ and the complementary probability $\tilde{q}(k) = 1 - \tilde{p}(k)$ of not yielding k counts. The probability of observing k counts r times out of M trials is given by a Binomial distribution function $B(r, M, \tilde{p}(k))$, where $\tilde{p}(k)$ is the probability to observe k counts. The expectation value $\langle r\rangle$ for the Binomial distribution is given by $\langle r\rangle = M\,\tilde{p}(k)$ and the standard deviation σ_k by $\sigma_k = \sqrt{M\,\tilde{p}(k)\,\tilde{q}(k)}$. We weigh each element of the PCH with its corresponding σ_k, calculate the theoretical density function $\Pi(k; \bar{N}, \epsilon)$ and then determine the reduced χ^2 function,

$$\chi^2 = M\frac{\sum_{k=k_{min}}^{k_{max}} \frac{(\tilde{p}(k) - \Pi(k; \bar{N}, \epsilon))^2}{\tilde{p}(k)\tilde{q}(k)}}{k_{max} - k_{min} - d}. \qquad (13)$$

The experimental photon counts range from a minimum value k_{min}, which is typically 0 for most experiments, to a maximum number k_{max}. The number of fitting parameters is given by d. Because we take on the order of $M = 10^6$ data points, the resulting Binomial distribution is, except for $\langle r\rangle \approx 1$, well approximated by a normal distribution. Thus, the quality of the model can be estimated by the reduced χ^2 and by the normalized residuals of the fit $r(k) = M\{[\tilde{p}(k) - \Pi(k; \bar{N}, \epsilon)]/\sigma_k\}$.

RESULTS

Resolvability analysis

We consider the most challenging case regarding a mixture of two species in which the molecular brightness and the concentrations of both species must be resolved by the histogram alone without any additional knowledge. It is quite useful, before taking data, to consider the influence of the molecular brightness and the particle concentration on the resolvability of two species. To address this question, we calculated histograms for different conditions to identify experimentally favorable concentrations and brightness conditions. The theoretically determined two-species PCH functions $\Pi(k; \bar{N}_1, \bar{N}_2, \epsilon_1, \epsilon_2)$ were fit assuming a single species model. The reduced χ^2_δ for this fit,

$$\chi^2_\delta = \underset{\{\bar{N},\,\epsilon\}}{\mathrm{Min}} \frac{\sum_{k=k_{min}}^{k_{max}} \left(M \dfrac{\Pi(k; \bar{N}_1, \bar{N}_2, \epsilon_1, \epsilon_2) - \Pi(k; \bar{N}, \epsilon)}{\sigma_k} \right)^2}{k_{max} - k_{min} - d}, \tag{14}$$

gives a measure of our ability to distinguish the PCH of one- and two-species systems. A fit of a two-species histogram by a single-species model will result in a misfit, which gives rise to systematic residuals. The magnitude and correlation of the residuals tells us whether it is feasible to distinguish between single and multiple species. Here, we only consider resolvability based on the value of the reduced χ^2_δ; but, in principle, other criteria for resolvability can be used as well. A reduced χ^2_δ value of one or less indicates that the data statistics are not sufficient to resolve the species, whereas a χ^2_δ greater than one indicates that more than one species is present. To study the concentration dependence of the two-species resolvability, we kept the molecular brightness values constant, but varied the particle concentrations systematically. For such a fixed brightness ratio, the results are best represented graphically in the form of a contour plot of the χ^2_δ surface as a function of the logarithmic concentration of both species. The concentration of each species is expressed in number of molecules within the PSF.

Figure 1 shows the χ^2_δ contour plot based on $M = 1.6 \times 10^7$ data samples for a molecular brightness of $\epsilon_A = 1.5$ for species A and $\epsilon_B = 6.0$ for species B, which gives a brightness ratio $r_\epsilon = \epsilon_B/\epsilon_A$ of 4. This corresponds to a radiative rate $\epsilon_{sec} = 30{,}000$ and 120,000 cpsm for a sampling time of $\Delta t_s = 50\ \mu$s per data point. Approximately 13 minutes are required to accumulate $M = 1.6 \times 10^7$ samples. As can be seen from Fig. 1, an optimal concentration for species A and species B exists, where the misfit of the two-species histogram by a single-species model is maximal. Changing the concentration of either species in either direction results in a decrease of this deviation, thus reducing the χ^2_δ value. Once the reduced χ^2_δ value is close to 1 or lower, then the signal statistics are not good enough to distinguish the presence of two species. The optimal average number of molecules for species A is close to 0.1 and the one for species B is about 0.02.

The shape of the χ^2_δ surface depends on the molecular brightness ratio, but is largely independent of the absolute brightness values, as indicated in Fig. 1. The dashed contour lines of χ^2_δ are plotted for the same brightness ratio, but with a difference in the absolute molecular brightness of a factor 6, $\epsilon_A = 0.25$ and $\epsilon_B = 1.0$. However, the amplitude of the χ^2_δ function strongly depends on the absolute molecular

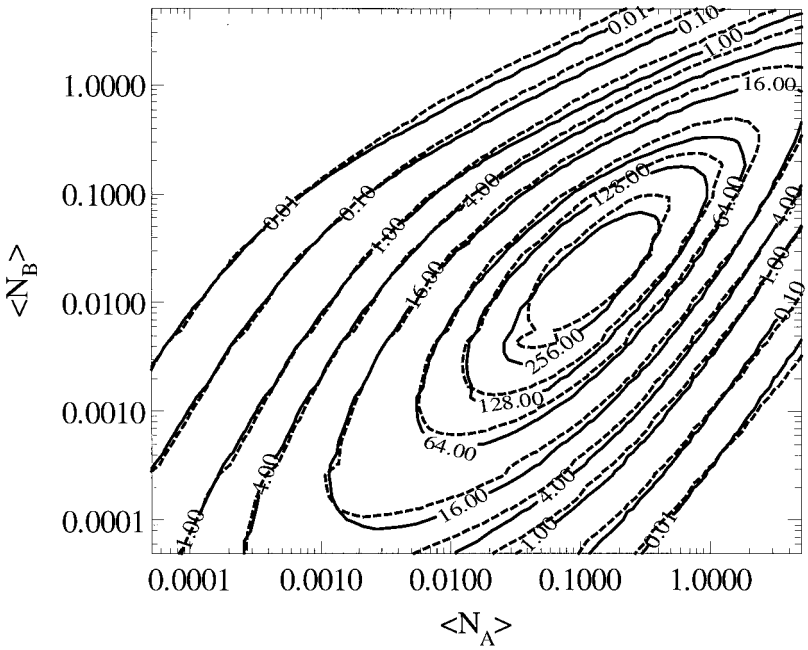

FIGURE 1 The χ^2_δ contour map of the misfit between a two-species PCH by a single-species PCH as a function of the logarithmic particle concentration. The solid contour lines represent the χ^2_δ surface for a brightness ratio of four, with molecular brightness values of $\epsilon_A = 1.5$ and $\epsilon_B = 6.0$. The maximal deviation between the double- and single-species PCH functions occurs approximately at a particle concentration of 0.1 for species A and 0.02 for species B. The dashed contour lines represent a rescaled χ^2_δ surface for another brightness ratio of four, but with molecular brightness values of $\epsilon_A = 0.25$ and $\epsilon_B = 1.0$. The χ^2_δ surface was calculated for $M = 1.6 \times 10^6$ data samples.

brightness values. The contour lines for the dimmer sample conditions are scaled by a factor of $6^{2.3}$ to match the χ^2_δ values of both mixtures.

To determine the dependence of χ^2_δ on the absolute molecular brightness, we varied ϵ_A systematically while keeping the brightness ratio r_ϵ constant. The dependence of χ^2_δ as a function of ϵ_A is shown in Fig. 2 *a* for a brightness ratio of 4 and for particle numbers of $\bar{N}_A = 1.0$ and $\bar{N}_B = 0.1$. The χ^2_δ function can be described approximately by a power law behavior for molecular brightness values, $\epsilon_A < 1$, with an exponent of about 2.4. For molecular brightness values, $\epsilon_A > 1$, we observe a convex shape of the χ^2_δ function on the doubly logarithmic plot. Thus, the slope of the curve gradually decreases from the value of 2.4 with increasing molecular brightness.

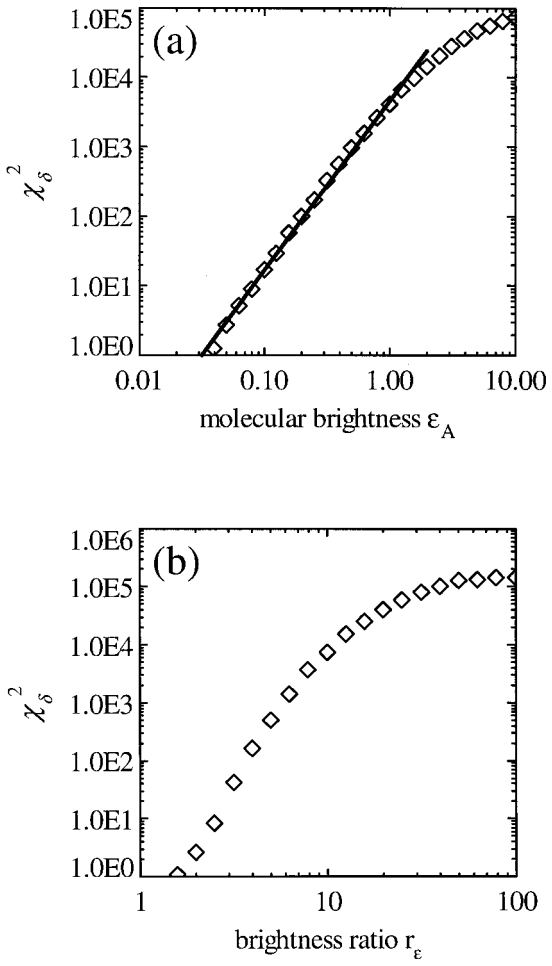

FIGURE 2 (*a*) χ^2_δ as a function of the molecular brightness ϵ_A. The χ^2_δ function was calculated according to Eq. 14 for particle numbers of 1.0 and 0.1 for species A and B, respectively. The brightness ratio $r_\epsilon = \epsilon_B/\epsilon_A$ was fixed to four during the calculations. The χ^2_δ values are shown in arbitrary units as symbols (◇) on a doubly logarithmic plot. A power law dependence of 2.4 (*solid line*) characterizes the initial influence of the molecular brightness ϵ_A on the χ^2_δ function. (*b*) χ^2_δ as a function of the molecular brightness ratio r_ϵ. The χ^2_δ function was determined for particle numbers of 1.0 and 0.1 for species A and B, respectively. The absolute molecular brightness of species A was fixed to $\epsilon_A = 0.1$ during the calculations of χ^2_δ, while the brightness ratio $r_\epsilon = \epsilon_B/\epsilon_A$ was varied. The χ^2_δ values are shown in arbitrary units as symbols (◇) on a doubly logarithmic plot.

So far, we have kept the molecular brightness ratio constant. However, it is the magnitude of the brightness ratio that provides the contrast between species. Clearly, a brightness ratio of 1 cannot be resolved, because both species have exactly the same molecular brightness. The larger the molecular brightness ratio is, the greater is the contrast between the two species. Thus, we expect a strong dependence of χ^2_δ on r_ϵ. We vary the brightness ratio r_ϵ from 1 to 100, while keeping the brightness of species A constant, $\epsilon_A = 0.1$. The number of particles is $\bar{N}_A = 1.0$ and $\bar{N}_B = 0.1$. The resulting χ^2_δ function is shown in Fig. 2 *b* on a doubly logarithmic plot. The curve initially has a steep slope for small brightness ratios, but that slope decreases steadily with increasing r_ϵ until the χ^2_δ function becomes independent of the molecular brightness ratio. The initial slope of the χ^2_δ function corresponds to an exponent of about 5. Since we are mainly interested in resolving small brightness ratios, the pronounced dependence of the signal statistics on the brightness ratio has profound consequences on the resolvability of small brightness differences between species.

Experimental verification of resolvability using a binary dye mixture

After considering the influence of the particle concentration and the molecular brightness on the signal statistics of the histogram, we study a binary dye mixture to demonstrate the feasibility of using PCH to resolve multiple species. A mixture of two dyes, rhodamine 110 and cyano-coumarin, was prepared. The mixture consisted of 80% coumarin and 20% rhodamine dye. The photon-count distribution of the binary mixture was determined and then analyzed by the PCH algorithm. One of the experimental histograms measured is shown in Fig. 3, together with the best fit to a single-species model. The deviation between the fit and the experimental histogram is clearly visible in the tail of the distribution. The residuals of the fit show systematic variations with standard deviations of more than 20 σ for several photon-count channels. The experimental PCH was then subject to a two-species fit. The two-species model describes the experimental PCH within statistical error. The residuals produced by the two-species fit are close to one and random (Fig. 3) and yield a reduced χ^2 of 0.8.

We performed a dilution experiment to check the accuracy of the PCH analysis. After each measurement of the binary dye mixture, the sample was diluted and remeasured. The concentration of each species is reduced by the dilution, but the concentration ratio is unaffected. The particle concentrations determined by PCH analysis from each measurement are plotted in Fig. 4 *a* together with the corresponding χ^2_δ surface similar to Fig. 1. The experimentally

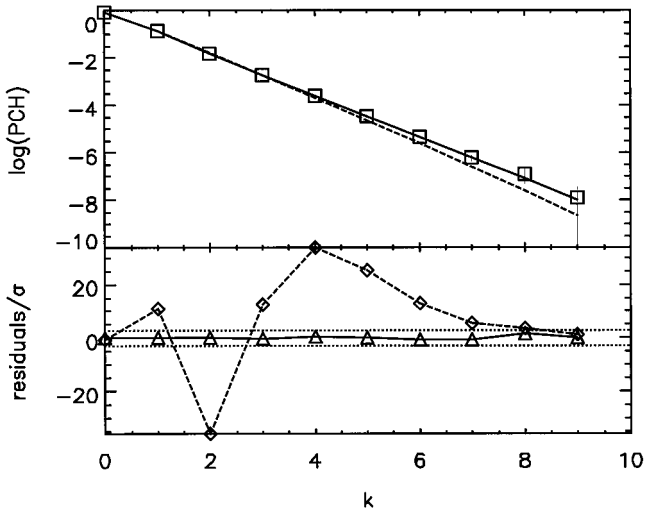

FIGURE 3 The PCH of a binary mixture of rhodamine and coumarin (□) is plotted together with the experimental error bar (±3 σ) for each data point. The dashed line represents a fit to a single-species model. The fit and the experimental PCH deviate in the tail of the distribution. The residuals of the single-species fit (*dashed line*) in the lower panel are correlated and exceed 20 SD for several photon count channels. A fit of the data to a two-species model (*solid line*) leads to a good description of the experimental histogram. The residuals (*solid line*) are random, and the reduced χ^2 for the two species fit is 0.8. The two dotted lines indicate the ±3 σ bounds.

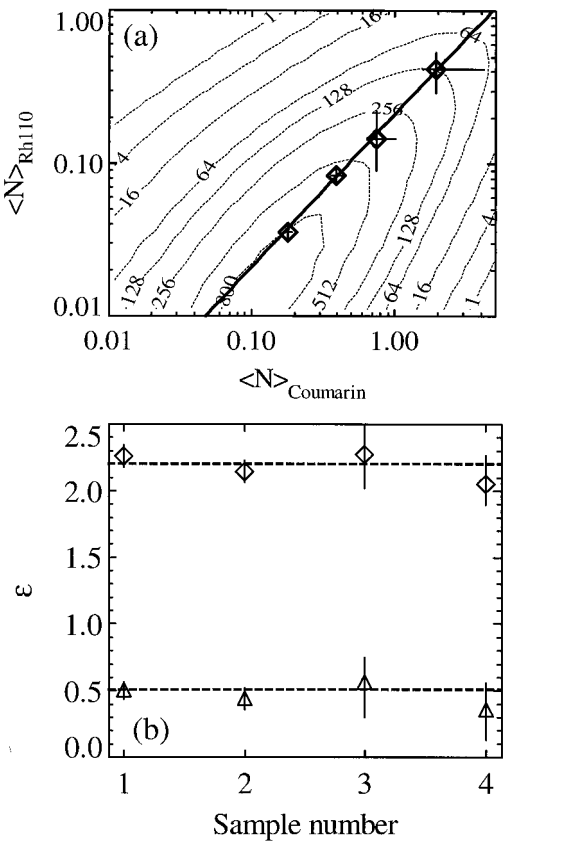

FIGURE 4 (*a*) A binary mixture of 20% rhodamine and 80% coumarin was diluted several times and the PCH of each dilution experimentally determined (see also Table 1). Each histogram was measured for 130 min and was then fit by a two-species model. The number of molecules recovered by the fit is shown in the χ^2 contour map (◇). The error bars associated with each data point correspond to 1 σ. The average value of the fitted molecular brightness of the rhodamine and the coumarin dye were used to calculate the χ^2_δ contour map for our experimental conditions. The contour lines are shown as dashed lines. The solid line represents the best approximation of the fitted dye concentrations by a dilution curve and corresponds to a composition of 17% rhodamine and 83% coumarin. (*b*) The fitted molecular brightness values are plotted together with their error bars (±1 σ) for the four samples measured. The mean of the molecular brightness of 0.47 and 2.18 for coumarin (△) and rhodamine (◇), respectively, are indicated by horizontal lines.

recovered numbers of particles were then used to determine the best concentration ratio describing the dilution experiment. This dilution curve is shown in Fig. 4 *a*, which describes a concentration ratio of 83%/17%, in excellent agreement with the expected concentration ratio. The particle concentrations determined from each individual histogram follow the dilution curve closely and do not scatter significantly. The 68% confidence interval (1 σ) of each particle concentration is shown in the form of error bars for each data point (see also Table 1).

The fitted molecular brightness values for the four different sample concentrations are shown in Fig. 4 *b* and in Table 1, together with their corresponding 68% confidence interval. For rhodamine, we determine an average molecular brightness of $\bar{\epsilon}_R = 2.18$ and, for coumarin, we get $\bar{\epsilon}_C = 0.47$. Thus, the brightness ratio of the rhodamine–coumarin pair is 4.6 for our experimental conditions. The molecular brightness values translate to 44,000 cpsm for rhodamine and 9400 cpsm for coumarin, because the data were collected with a sampling time of $\Delta t_s = 50$ μs.

Each dye mixture was remeasured with a data acquisition time that was ten times shorter than in the previous experiment. The statistical deviation from a single-species PCH is now reduced, and the values of the χ^2_δ (Eq. 14) are a factor of ten less than that for the data corresponding to the longer integration time. Note that the χ^2 function is proportional to M, the number of data points, and therefore proportional to the length of the data acquisition time. Fitting of the individual histograms is still possible, but with an increase in the uncertainty of the recovered parameters. To exploit the fact that the molecular brightness is independent of the dilution process, we fit the histograms globally by linking the brightness of the two dyes across the data sets, while allowing the dye concentrations to vary. The concentration pairs recovered by the global fit ($\chi^2 = 1.1$) are shown in Fig. 5, together with the best dilution curve describing the data points (*solid line*). From the dilution curve, we recover a composition of 81% coumarin and 19% rhodamine. The global fit returns a molecular brightness of $\epsilon_R = 2.2$ for rhodamine and $\epsilon_C = 0.5$ for coumarin.

TABLE 1 Resolution of binary dye mixture by PCH analysis

	Samples			
	4	3	2	1
ϵ_1	$0.51^{+0.064}_{-0.069}$	$0.45^{+0.077}_{-0.085}$	$0.56^{+0.19}_{-0.26}$	$0.36^{+0.21}_{-0.23}$
$\bar{N}_1$	$0.181^{+0.012}_{-0.008}$	$0.39^{+0.045}_{-0.026}$	$0.74^{+0.27}_{-0.055}$	$1.95^{+2.20}_{-0.38}$
ϵ_2	$2.26^{+0.088}_{-0.081}$	$2.14^{+0.088}_{-0.080}$	$2.27^{+0.32}_{-0.26}$	$2.05^{+0.22}_{-0.15}$
$\bar{N}_2$	$0.035^{+0.0047}_{-0.0044}$	$0.084^{+0.011}_{-0.011}$	$0.146^{+0.074}_{-0.056}$	$0.414^{+0.12}_{-0.12}$
χ^2	0.83	0.59	2.39	0.43

A binary dye mixture of 80% coumarin and 20% rhodamine 110 was diluted repeatedly and its PCH was determined. The data acquisition time for each histogram was 130 min during which a total of 1.6×10^8 data points were collected. Each histogram was fitted by a two-species model and the reduced χ^2 of the fit is reported. The recovered molecular brightness (ϵ_1 and ϵ_2) and the average number of molecules ($\bar{N}_1$ and $\bar{N}_2$) of each species are shown together with their respective 1 σ uncertainty (see also Fig. 4). The confidence interval of each parameter was determined by F-test analysis.

Experimental verification of resolvability using fluorescently labeled biomolecules

In the next step, we apply PCH analysis to biomolecules. To demonstrate that it is feasible to distinguish a brightness ratio of two, IgG antibodies and alcohol dehydrogenase were labeled with the fluorescent dye alexa 488. The labeling process generates a heterogeneous mixture of proteins, which differ in the number of fluorophores attached. Cold proteins, protein molecules without a label, do not contribute to the fluorescence signal and will be ignored. In the first preparation, the labeling conditions for the two proteins were chosen, so that, besides cold proteins, only proteins with a single label are present. In the second preparation, the amount of dye was increased, so that an additional doubly-labeled protein species appeared. Both preparations of alcohol dehydrogenase were measured and their histograms analyzed (Table 2). The PCH of the first preparation of alcohol dehydrogenase (sample A) is plotted in Fig. 6 *a*, together with the fit to a single species, which represents the data within statistical error. The corresponding PCH of the second preparation (sample B) requires a fit to a two-species model (Fig. 6 *b*). The molecular brightness ratio of the two species obtained by the PCH fit of the second sample is 2.2, which is within statistical error of the expected value of two for the brightness difference between a singly and doubly labeled protein. Furthermore, the brightness ratio of the first species across the two independently measured samples equals 1.04. The fact that we recover essentially the same molecular brightness for species from independent measurements together with the brightness ratio of about 2 of the second sample is a good indication that we can indeed resolve a mixture of singly and doubly labeled proteins by the histogram method.

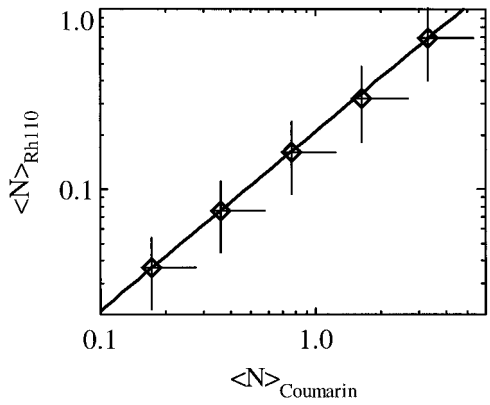

FIGURE 5 Global analysis of a binary dye mixture containing 20% rhodamine and 80% coumarin. The mixture was diluted several times and the PCH of each dilution was measured for 13 min. The PCHs were simultaneously fit to two-species models with the molecular brightness of each species linked across the data sets. The reduced χ^2_δ of the fit is 1.1. The global fit yields a molecular brightness of $\epsilon_R = 2.2$ for rhodamine and $\epsilon_C = 0.5$ for coumarin. The concentration pairs of the dyes recovered from the fit are displayed together with their error bars ($\pm 1\ \sigma$) as determined by the F-test criterion. The concentration points are best described by a dilution curve of 81% coumarin and 19% rhodamine (*solid line*).

We successively increased the ratio of dye to protein in the labeling reaction to generate proteins with more than two fluorophores attached. To resolve such a mixture into its components, we use a global analysis similar to the one used for the binary dye mixtures. Each additional species needed in the global PCH fit has to be an integer multiple of the molecular brightness of the single-labeled species, where the integer represents the number of dyes attached to the protein. We applied this model to three PCHs of labeled IgG samples. The data are well described by the global model, which yields a reduced χ^2 of 2.5, and the result of the fit is shown in Table 3, together with the 68% confidence intervals of the fitted parameters. The molecular brightness of the singly labeled species is 1.7. The histogram of the first sample is fit by a single species and the histogram of the second sample requires a fit to a two-species model. The third protein sample, however, is not described by two species alone and a third component, which carries three fluorescent labels, had to be included (Table 3). The concentration of the higher label fractions decreases rapidly with the number of dyes attached, as one would expect from random labeling.

TABLE 2 Resolution of alcohol dehydrogenase labeled with alexa 488 by PCH analysis

Samples	ϵ_1	$\bar{N}_1$	ϵ_2	$\bar{N}_2$	χ^2
A	$2.62^{+0.019}_{-0.018}$	$0.540^{+0.0036}_{-0.0039}$	—	—	0.75
B	$2.51^{+0.06}_{-0.12}$	$0.155^{+0.007}_{-0.002}$	$5.6^{+1.0}_{-1.0}$	$0.006^{+0.008}_{-0.003}$	1.82

Two protein samples were labeled with different concentrations of alexa 488 as discussed in the text. The PCH of the first sample (sample A) is fitted within statistical error by a single-species model, whereas sample B required a fit to a two-species model to describe the data within statistical error. The recovered molecular brightness and the number of molecules are shown together with their respective 1 σ standard deviation. The data acquisition time of sample A and B was 13 and 130 min, respectively.

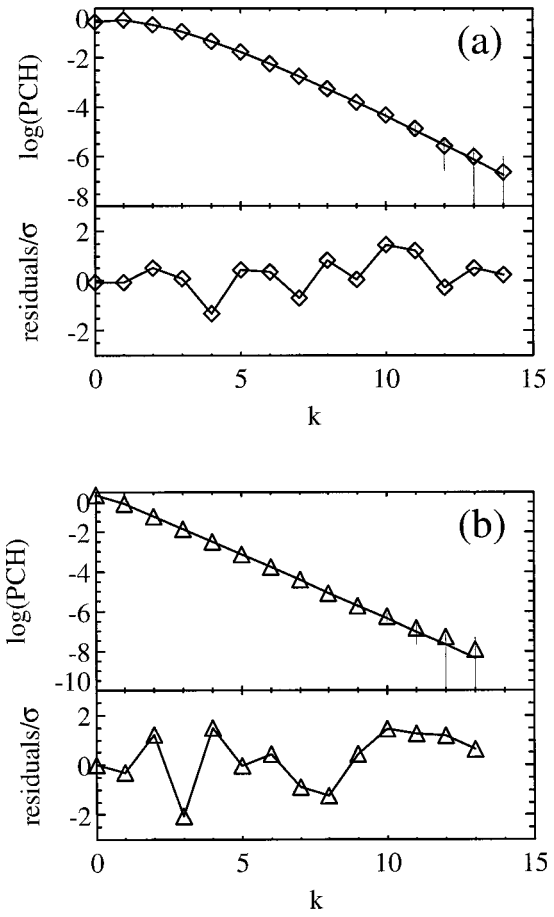

FIGURE 6 PCHs of alcohol dehydrogenase labeled with alexa 488. (*a*) The PCH (◇) of a singly labeled protein (sample A of Table 2) is fit to a single-species model (*solid line*), and the normalized residuals of the fit are shown in the lower panel. (*b*) The PCH (△) of a mixture of singly and doubly labeled protein (sample B of Table 2) is fit to a two-species model (*solid line*). The normalized residuals of the fit are shown in the lower panel. The fit parameters for both histograms are compiled in Table 2.

We increased the labeling ratio even further and had to include a forth species to describe the data. However, the χ^2 of that and other data sets from samples with higher labeling ratios is increasing steadily. This indicates that the global model, which assumes that the brightness scales with the number of attached fluorophores, starts to fail in describing the experimental situation. The most likely explanation for this deviation between data and fit is that the labeling ratio starts to be high enough so that quenching between the labeled fluorophores becomes important. For alcohol dehydrogenase the deviation begins already at a labeling ratio lower than for IgG.

DISCUSSION

The PCH of multiple independent species is the convolution of the PCH of each individual species. Each species in the histogram is uniquely characterized by two parameters, the molecular brightness and the average number of particles in the observation volume as outlined in the theory section. The practical resolvability of the individual species depends on the shape of the χ^2_δ function and on the signal statistics of the experimentally determined histogram. We examined the resolvability of two species in detail, where all four parameters must be determined directly from the histogram. The histogram obtained from a sample of a mixture must be sufficiently different from any single species histogram to resolve the two components in terms of concentration and brightness. This difference is quantitatively expressed by the χ^2_δ function defined by Eq. 14. A χ^2_δ value sufficiently higher than one is a clear indication that more than one species is present.

The χ^2_δ surface of Fig. 1 demonstrates that, for a given brightness ratio $r_\epsilon = \epsilon_B/\epsilon_A$, an optimal concentration for species A and B exists at which the deviation from a single-species PCH is maximized. An increase or decrease in the particle concentration from the optimal concentration leads to a reduction of the χ^2_δ value. We can understand this behavior readily by considering the influence of the concentration of a single species on the intensity fluctuations. If we increase the number of molecules in the observation volume, then we simultaneously decrease the relative contribution of the number fluctuations to the signal. Thus, the relative width of the particle number distribution (Eq. 6) narrows as the concentration grows, and the number distribution approaches a delta function $\delta(N - \bar{N})$ for high particle concentrations. The intensity fluctuations associated with the particle number die away and the PCH approaches a Poisson distribution according to Mandel's formula (Chen et al., 1999). However, it is the deviation of the PCH from a Poisson distribution, which allows us to determine both the molecular brightness and the number of molecules, as discussed by Chen et al. (1999). Consequently, the signal statistics decrease as the particle concentration is increased.

TABLE 3 Global PCH analysis of IgG labeled with alexa 488

	Samples		
	A	B	C
$\bar{N}_1$	$0.234^{+0.003}_{-0.003}$	$0.245^{+0.005}_{-0.005}$	$0.26^{+0.03}_{-0.03}$
$\bar{N}_2$	—	$0.031^{+0.004}_{-0.004}$	$0.08^{+0.03}_{-0.03}$
$\bar{N}_3$	—	—	$0.03^{+0.01}_{-0.01}$

Three samples of IgG labeled with alexa 488 were prepared as described in the text. The relative dye concentration used for the labeling reaction increased from sample A to sample C. The global model assumes that the molecular brightness scales with the number of fluorophores linked to the protein. The reduced χ^2 of the global fit is 2.5 and the fitted molecular brightness of the singly labeled protein is $\epsilon = 1.7$. The average number of molecules of proteins ($\bar{N}_1$, $\bar{N}_2$, and $\bar{N}_3$) with a single, with two, and with three labels is tabulated together with their 1 σ SD. The data acquisition time used to determine the PCH was 800 s for each sample.

Reducing the number of molecules in the observation volume, in contrast, produces stronger fluctuation amplitudes. However, once the average number of molecules is less than one molecule, the probability that a molecule is found in the observation volume greatly decreases. Therefore, most of the time, the particle will not contribute to the photon count signal, which consequently leads to a reduction of the signal-to-noise ratio. The two opposing effects of the particle concentration on the signal statistics shape the χ^2 function and lead to a maximum at a concentration of about one molecule per observation volume. A brighter particle shifts the maximum of the χ^2 function to a lower concentration than that when compared to the case of a dimmer particle. In other words, the exact location of the optimal concentration conditions depends on the relative brightness ratio of the two species. However, on a doubly logarithmic plot, the optimal position does not shift appreciably with these changes. Thus, concentrations of one particle per observation volume or slightly lower are good experimental conditions for separating species by the PCH algorithm.

If one must work at conditions where the χ^2_δ value is low, one can increase the signal to noise by choosing a longer data acquisition time. As can be seen from Eq. 13, the value of χ^2 is directly proportional to M, the number of data points collected. Thus, one can judge, for given experimental conditions, how long of a data acquisition time is needed to identify the second species.

The shape of the χ^2_δ surface is largely independent of the absolute molecular brightness as indicated in Fig. 1, as long as the brightness ratio is kept constant. The absolute value of χ^2_δ, however, depends strongly on the absolute brightness (Fig. 2 *a*). We have shown previously that, for a single species, the deviation of the photon counting histogram from a Poisson distribution increases with the molecular brightness (Chen et al., 1999). Similarly, the signal statistics required to separate species improves as the molecular brightness is raised. The dependence of the χ^2_δ on the absolute molecular brightness is approximately described by a power law with an exponent of 2.4 for brightness values $\epsilon_A < 1$. The value of the exponent decreases only slightly with increasing brightness ratio r_ϵ (data not shown).

The PCH of a binary mixture is the convolution of the corresponding single-species histograms. The resolution of the molecular brightness values from the histogram depends on the relative overlap of the two histograms. For small molecular brightness values, the shot noise broadening of the histogram is significant. However, the separation of the average photon counts of both species increases as the molecular brightness is raised, while, at the same time, the relative shot noise broadening is reduced. Thus, the two distributions are better separated as the brightness is increased. As we continue to increase the molecular brightness, the contribution of the shot noise to the signal decreases rapidly, and the measured signal is directly proportional to the fluorescence intensity. As we cross from the regime, where the shot noise contribution is important, to the intensity limit, the signal statistics to separate species will change. The molecular brightness ϵ determines the average photon counts per molecule and sampling time. Thus, then $\epsilon \gg 1$ the contribution of the shot noise becomes negligible and we approach the intensity limit. This effect explains the decrease of the slope in Fig. 2 *a* as the influence of the shot noise becomes less important.

For our experimental conditions, the shot noise influence upon the data statistics is important. Thus, the power law behavior with an exponent of close to two is a good approximation to judge the influence of the absolute brightness on the signal statistics. For example, a decrease of the absolute brightness by a factor of two requires a data acquisition time that is approximately $2^{2.4}$ times longer, to yield the same χ^2_δ value.

Another important factor to consider is the brightness ratio. The brightness ratio gives us the contrast to distinguish between species. The signal statistics presented in Fig. 2 *b* clearly reflect this behavior. As the contrast between the two species increases, so does the χ^2_δ deviation from a single species fit. However, as the brightness ratio is progressively increased, the logarithmic slope of the χ^2_δ curve decreases until the χ^2_δ value becomes independent from the brightness ratio r_ϵ. The initial increase of the signal statistics can be understood in terms of an increase of the separation of the individual histograms, as in the previously discussed case of the absolute brightness dependence. The overlap of the individual PCH decreases to the point that they are virtually separate. At this point, a further increase in the molecular brightness will not lead to a significant improvement of the ability to separate the species. This behavior can explain the decrease and eventual saturation of the χ^2_δ dependence as a function of the brightness ratio r_ϵ. In fact, at extremely high brightness ratios, the bright species will almost exclusively contribute to the photon count signal, while the counts from the dimmer species are negligible. Therefore, the signal statistics will actually decrease above a certain brightness contrast. However, in almost all practical applications, the brightness ratio will be on the order of ten or less. The shape of the χ^2_δ curve as a function of the brightness ratio depends on the particle concentration ($\bar{N}_A$ and $\bar{N}_B$), because the optimal concentration changes with the brightness ratio. However, the overall shape stays the same; a straight slope in a doubly logarithmic plot, which decreases with increasing brightness ratio. The steep slope of the curve in the doubly logarithmic plot explains why it is so much harder to separate smaller brightness ratios. For example, changing the brightness ratio from 4 to 2 for particle concentrations of $\bar{N}_A = 1.0$ and $\bar{N}_B = 0.1$, reduces the χ^2_δ by a factor of 2^5. Thus, the data acquisition time has to be increased by a factor of 30 to compensate for the loss in the signal statistics.

The study of the influence of the molecular brightness and the particle concentration on the value of χ^2_δ tells us

whether, statistically, more than one species is present, but does not tell us how accurately the mixture is resolved into its components. In real experiments, we need to determine the confidence interval of the parameters recovered by the fit, which we do by using the F-test criterion to judge the accuracy of the fit parameters.

We studied a binary dye mixture at the single-molecule level and used PCH analysis to separate the species (Fig. 4 and Table 1). Each histogram was acquired for 130 min. The highest dilution has the best signal-to-noise ratio and the standard deviation of the parameters is 10% or less. As we increase the concentration, the uncertainty in the parameters increases. This exactly reflects the behavior predicted from the study of the χ^2_δ dependence on the particle concentration. With increasing particle concentration, the statistical deviation of the two-species histogram from a single-species PCH decreases, as can be seen from the contour lines in Fig. 4 *a*. To compensate for the loss in resolvability, a longer data integration time would be necessary. The PCH analysis of the dilution study clearly demonstrates that two species can be separated based on a brightness difference. The autocorrelation function, in contrast, will not be able to distinguish the species, because the diffusion coefficient of the two dyes is virtually identical.

We like to stress that the analysis of the binary dye data is based on a single histogram assuming no additional information about the molecular brightness or the particle concentration of each species. This is by far the most stringent condition and is chosen to illustrate the experimental strength of the PCH analysis. To the best of our knowledge, this is the first demonstration that a mixture can be resolved on the single-molecular level by a brightness difference alone. Previous studies based on higher order autocorrelation techniques and moment analysis used the intensity or photon count moments to separate species (Qian and Elson, 1990b; Palmer and Thompson, 1987). The moments like the PCH contain information about the molecular brightness of particles and can be used to resolve a mixture of species. However, in all previous studies, the signal statistics were insufficient to directly resolve the species, and either the brightness or the concentration of one of the species was determined by some additional experiment (Palmer and Thompson, 1989a; Qian and Elson, 1990a).

Reducing the data acquisition time leads to an increase in the parameter uncertainty. However, one can compensate for a shortened data acquisition time by either increasing the molecular brightness or by using global analysis techniques. The same binary dye mixtures were remeasured with a data acquisition time of only 13 minutes per sample. The complete set of PCHs was analyzed globally by linking the molecular brightness of each species across the data sets. By performing a global analysis, we were able to recover the molecular brightness of the two dyes and their concentrations at a reduced data acquisition time.

FCS is used to characterize kinetic properties of biomolecules on the single-molecule level. Most biological systems contain more than one chemical species. As already pointed out in the introduction, FCS cannot differentiate between mixtures of similar molecular weight. Here, PCH can fill an important gap in the characterization of biological systems on the single-molecule level. As discussed earlier, the resolvability of two species decreases as the brightness contrast is reduced. The question, whether one can resolve a brightness ratio of two, is of imminent biological importance. Biomolecules often build complex structures, composed of many individual units, to fulfill a specific task. The ribosomes are but one such example. The fundamental building block is the assembly of two units. If each unit is labeled, then the brightness increase of the duplex is a factor of two. We experimentally verified that a brightness ratio of two can be resolved by studying fluorescently labeled proteins (see Fig. 6). The two species recovered only differ in the number of dyes attached to the protein. Therefore, lifetime measurements or dual-color FCS (Schwille et al., 1997) cannot be used to resolve the heterogeneous protein sample.

We globally analyzed three histograms of IgG labeled with the fluorophore alexa to reduce the data acquisition time substantially and to illustrate the power of PCH analysis. Our model assumes that the molecular brightness scales with the number of fluorophores linked to the protein. The model fits the data, and we can isolate up to three species (Table 3). If we assume that the unspecific labeling reaction is truly random, or, in other words, the probability for a label to bind to the protein is independent of the number of fluorophores already attached to the protein, then we would expect to find a Poisson distribution for the number of labeled fluorophores. This assumption might hold for large proteins and small labeling ratios. We analyzed the concentrations recovered by the fit for the protein samples B and C assuming a Poisson distribution (data not shown). From the fit, we estimate a labeling ratio of 0.2 for sample B and a labeling ratio of 0.8 for sample C, which is in excellent agreement with the dye-to-protein ratio used in the labeling reaction (see Materials and Methods).

Two other approaches to recover multiple species have been introduced in the literature. One method is based on the analysis of higher order autocorrelation functions (Palmer and Thompson, 1987, 1989a,b) and the other method is based on moment analysis of the photon counts (Qian and Elson, 1989, 1990a,b). The analysis of the higher order autocorrelation function determines the higher order fluctuation amplitude, which is a function of the intensity moments. Thus, both methods use moments to resolve species. In principle, higher order autocorrelation analysis could exploit the information content of the time-dependence of the higher order intensity fluctuations to separate species, but its potential use still has to be demonstrated. From a purely mathematical point of view, histogram and

moment analysis are equivalent, because the knowledge of all moments is equivalent to the knowledge of the distribution function of the photons. However, the statistical error affects the intensity moments and the histogram differently. A simple, analytical form describes the statistical error of PCH, and this error is taken into account in the PCH analysis. This allows us to fit data to models and judge the quality of the fit from the residuals and the reduced χ^2 in a quantitative manner. The transformation of the simple expression for the error of PCH analysis to moments is quite complex. In fact, the statistical uncertainty has not been determined analytically. But moment analysis based on shot-noise subtraction can be extremely fast and convenient, because it determines the molecular brightness and the average number of molecules by direct calculation, instead of using a nonlinear least squares fit (Qian and Elson, 1990b).

Moment analysis is confronted with the problem of how many moments to include in the analysis. Until a statistical criterion is found, such a decision is, to a certain degree, arbitrary. In fact, a previous study included the fourth moment only to conclude later in the paper that it does not provide accurate information (Palmer and Thompson, 1989a). PCH, in contrast, is free from such arbitrary decisions. All elements of the histogram are accounted for together with their proper statistical weight. Thus, PCH uses all the information available from the histogram.

The method of PCH analysis lends itself to global analysis. In this contribution, we demonstrated analysis of PCHs by a global model. However, one can link PCH analysis with any other experimental technique. A combined analysis of the autocorrelation function and PCH is an interesting application. Consider a mixture of two components, which differ slightly in their diffusion coefficients and their molecular brightness values. Analyzing the mixture by either the autocorrelation or the PCH method alone might not be sufficient to resolve the mixture. However, a global analysis using both methods should almost certainly increase the sensitivity to resolve the species.

CONCLUSIONS

PCH is sensitive to the brightness of particles; thus offering the possibility to distinguish between a mixture of species based on brightness alone. The resolvability of these species depends on the signal statistics of the histogram. We demonstrated that, for mixtures of two species with a given brightness contrast, a concentration of about one particle per observation volume is optimal for the resolution of each component by the histogram method. We demonstrated the method experimentally by successfully resolving a binary dye mixture from a single PCH without any additional knowledge. To demonstrate the feasibility of PCH analysis, each histogram was measured and analyzed for the same dye composition at different dilutions. The recovered molecular brightness and the concentration of each species changed as expected, and we retrieved the fractional composition of the mixture within experimental error. We extended PCH analysis to biomolecules, where we resolved protein samples with either one or two fluorescent labels attached. Our demonstration, that a brightness ratio of two is experimentally resolvable, is of importance for biological applications. The association of two labeled monomeric units to form a dimer changes the brightness by a factor of two, whereas the diffusion coefficient only increases by 25%, which cannot be resolved by the autocorrelation function alone. These examples demonstrate the potential power of PCH in fluorescence fluctuation experiments. PCH characterizes the amplitude distribution of fluorescence intensity fluctuations, whereas the autocorrelation function describes the time dependence of these fluctuations. Thus, PCH and FCS provide complementary information for resolving multiple species, which should prove useful in tackling biological problems with fluorescence fluctuation spectroscopy.

REFERENCES

Abramowitz, M., and I. A. Stegun. 1965. Handbook of Mathematical Functions with Formulas, Graphs, and Mathematical Tables. Dover Publications, New York. 260–263.

Berland, K. M., P. T. C. So, Y. Chen, W. W. Mantulin, and E. Gratton. 1996. Scanning two-photon fluctuation correlation spectroscopy: particle counting measurements for detection of molecular aggregation. *Biophys. J.* 71:410–420.

Berland, K. M., P. T. C. So, and E. Gratton. 1995. Two-photon fluorescence correlation spectroscopy: method and application to the intracellular environment. *Biophys. J.* 68:694–701.

Bonnet, G., O. Krichevsky, and A. Libchaber. 1998. Kinetics of conformational fluctuations in DNA hairpin-loops. *Proc. Natl. Acad. Sci. USA.* 95:8602–8606.

Borejdo, J. 1979. Motion of myosin fragments during actin-activated ATPase: fluorescence correlation spectroscopy study. *Biopolymers.* 18: 2807–2820.

Chandrasekhar, S. 1943. Stochastic problems in physics and astronomy. *Rev. Mod. Phys.* 15:1–89.

Chen, Y., J. D. Müller, P. T. C. So, and E. Gratton. 1999. The photon counting histogram in fluorescence fluctuation spectroscopy. *Biophys. J.* 77:553–567.

Ehrenberg, M., and R. Rigler. 1974. Rotational Brownian motion and fluorescence intensity fluctuations. *Chem. Phys.* 4:390–401.

Eigen, M., and R. Rigler. 1994. Sorting single molecules: application to diagnostics and evolutionary biotechnology. *Proc. Natl. Acad. Sci. USA.* 91:5740–5747.

Elson, E. L., and D. Magde. 1974. Fluorescence correlation spectroscopy. I. Conceptual basis and theory. *Biopolymers.* 13:1–27.

Feller, W. 1957. An Introduction to Probability Theory and Its Applications. Vol. 1. John Wiley & Sons, Inc., New York. 250–253.

Haupts, U., S. Maiti, P. Schwille, and W. W. Webb. 1998. Dynamics of fluorescence fluctuations in green fluorescent protein observed by fluorescence correlation spectroscopy. *Proc. Natl. Acad. Sci. USA.* 95: 13573–13578.

Huang, Z., and N. L. Thompson. 1996. Imaging fluorescence correlation spectroscopy: nonuniform IgE distributions on planar membranes. *Biophys. J.* 70:2001–2007.

Klingler, J., and T. Friedrich. 1997. Site-specific interaction of thrombin and inhibitors observed by fluorescence correlation spectroscopy. *Biophys. J.* 73:2195–2200.

Koppel, D. E., D. Axelrod, J. Schlessinger, E. L. Elson, and W. W. Webb. 1976. Dynamics of fluorescence marker concentration as a probe of mobility. *Biophys. J.* 16:1315–1329.

Magde, D. 1976. Chemical kinetics and fluorescence correlation spectroscopy. *Q. Rev. Biophys.* 9:35–47.

Magde, D., E. Elson, and W. W. Webb. 1972. Thermodynamic fluctuations in a reacting system: measurement by fluorescence correlation spectroscopy. *Phys. Rev. Lett.* 29:705–708.

Magde, D., E. L. Elson, and W. W. Webb. 1974. Fluorescence correlation spectroscopy. II. An experimental realization. *Biopolymers.* 13:29–61.

Magde, D., W. W. Webb, and E. L. Elson. 1978. Fluorescence correlation spectroscopy. III. Uniform translation and laminar flow. *Biopolymers.* 17:361–376.

Mandel, L. 1958. Fluctuations of photon beams and their correlations. *Proc. Phys. Soc.* 72:1037–1048.

Meseth, U., T. Wohland, R. Rigler, and H. Vogel. 1999. Resolution of fluorescence correlation measurements. *Biophys. J.* 76:1619–1631.

Palmer, A. G., III, and N. L. Thompson. 1987. Molecular aggregation characterized by high order autocorrelation in fluorescence correlation spectroscopy. *Biophys. J.* 52:257–270.

Palmer, A. G., III, and N. L. Thompson. 1989a. High-order fluorescence fluctuation analysis of model protein clusters. *Proc. Natl. Acad. Sci. USA.* 86:6148–6152.

Palmer, A. G., III, and N. L. Thompson. 1989b. Intensity dependence of high-order autocorrelation functions in fluorescence correlation spectroscopy. *Rev. Sci. Instrum.* 60:624–633.

Qian, H., and E. L. Elson. 1989. Characterization of the equilibrium distribution of polymer molecular weights by fluorescence distribution spectroscopy (theoretical results). *In* Applied Polymer Symposia. John Wiley & Sons Inc., New York. 305–314.

Qian, H., and E. L. Elson. 1990a. Distribution of molecular aggregation by analysis of fluctuation moments. *Proc. Natl. Acad. Sci. USA.* 87: 5479–5483.

Qian, H., and E. L. Elson. 1990b. On the analysis of high order moments of fluorescence fluctuations. *Biophys. J.* 57:375–380.

Qian, H., and E. L. Elson. 1991. Analysis of confocal laser-microscope optics for 3-D fluorescence correlation spectroscopy. *Appl. Opt.* 30: 1185–1195.

Rauer, B., E. Neumann, J. Widengren, and R. Rigler. 1996. Fluorescence correlation spectrometry of the interaction kinetics of tetramethylrhodamin alpha-bungarotoxin with *Torpedo californica* acetylcholine receptor. *Biophys. Chem.* 58:3–12.

Rigler, R., Ü. Mets, J. Widengren, and P. Kask. 1993a. Fluorescence correlation spectroscopy with high count rate and low background: analysis of translational diffusion. *Eur. Biophys. J.* 22:169–175.

Rigler, R., J. Widengren, and Ü. Mets. 1993b. Interactions and kinetics of single molecules as observed by fluorescence correlation spectroscopy. *In* Fluorescence Spectroscopy: New Methods and Applications. O. S. Wolfbeis, editor. Springer, Berlin. 13–24.

Saleh, B. 1978. Photoelectron Statistics, with Applications to Spectroscopy and Optical Communications. Springer-Verlag, Berlin.

Schwille, P., F. J. Meyer-Almes, and R. Rigler. 1997. Dual-color fluorescence cross-correlation spectroscopy for multicomponent diffusional analysis in solution. *Biophys. J.* 72:1878–1886.

Thompson, N. L. 1991. Fluorescence correlation spectroscopy. *In* Topics in Fluorescence Spectroscopy. J. R. Lakowicz, editor. Plenum, New York. 337–378.

Thompson, N. L., and D. Axelrod. 1983. Immunoglobulin surface-binding kinetics studied by total internal reflection with fluorescence correlation spectroscopy. *Biophys. J.* 43:103–114.

Weissman, M., H. Schindler, and G. Feher. 1976. Determination of molecular weights by fluctuation spectroscopy: application to DNA. *Proc. Natl. Acad. Sci. USA.* 73:2776–2780.

Widengren, J., Ü. Mets, and R. Rigler. 1995. Fluorescence correlation spectroscopy of triplet states in solution—a theoretical and experimental study. *J. Phys. Chem.* 99:13368–13379.